World Journal of Condensed Matter Physics, 2012, 2, 181-187
http://dx.doi.org/10.4236/wjcmp.2012.24030 Published Online November 2012 (http://www.SciRP.org/journal/wjcmp)

Synthesis and Magnetic Properties of $Ba_2Ni_{2-x}Zn_xFe_{12}O_{22}$ Hexaferrites

Sajal Chandra Mazumdar[1*], A. K. M. Akther Hossain[2]

[1]Department of Physics, Comilla University, Comilla, Bangladesh; [2]Department of Physics, Bangladesh University of Engineering and Technology, Dhaka, Bangladesh.
Email: *sajalf@yahoo.com

Received July 29th, 2012; revised August 30th, 2012; accepted September 9th, 2012

ABSTRACT

Y-type hexagonal ferrites with the nominal chemical composition $Ba_2Ni_{2-x}Zn_xFe_{12}O_{22}$ ($0.0 \le x \le 0.6$ with a step of 0.1) have been synthesized by the conventional solid state reaction method and sintered in the temperature range 1150˚C - 1250˚C to study their structural and magnetic properties. The aim of the present work is to increase the magnetic properties of Y-type hexaferrites by Zn substitution. X-ray diffraction analysis confirms the formation of the hexagonal phase. The effect of chemical composition on the lattice parameter, density and porosity is studied. The lattice parameter increases with Zn substitution. The density increases with Zn substitution up to a certain level and after that density decreases. The ac magnetic properties of the hexaferrites sintered at temperature 1200˚C are characterized within the frequency range 100 kHz - 120 MHz. The real part (μ_i') of the complex initial permeability for different compositions indicates that μ_i' decreases with increase in frequency. The permeability increases with the increase in Zn content, reaches a maximum value and then decreases with further increase in Zn content. Magnetization has been measured using the Superconducting Quantum Interference Device (SQUID) magnetometer. The saturation magnetization is observed to be maximum at $x = 0.1$ and then decreases with Zn content for $x > 0.1$. From the *M-H* curve it is clear that at room temperature the polycrystalline $Ba_2Ni_{2-x}Zn_xFe_{12}O_{22}$ compositions are in ferrimagnetic state.

Keywords: Hexagonal Ferrites; X-Ray Diffraction; Porosity; Permeability; Magnetization

1. Introduction

Ferrites have continued to attract attention over years. As magnetic materials, ferrites cannot be replaced by any other magnetic material because they are relatively inexpensive, stable and have a wide range of technological applications in transformer core, high quality filters, high and very high frequency circuits and operating devices [1]. The physical properties of ferrites are controlled by the preparation conditions, chemical composition, sintering temperature and time, type and amount of substitutions [2]. The increasing exploitation of microwave (MW) frequencies for telecommunications has increased electromagnetic (EM) interference and pollution and stimulated the development of MW absorbers. Absorption of EM waves occurs in magnetic materials due to the magnetic losses. Ferrite materials have been observed to exhibit substantial losses in the vicinity of ferromagnetic resonance (FMR) and dipole relaxation peak. The spinel ferrites can be used only up to 3 GHz frequency range, but the hexaferrites can be used in the whole GHz region due to their intrinsic uniaxial anisotropic property. The hexaferrites are ferrites with complex crystal structure of $AO\text{-}Fe_2O_3\text{-}MeO$ (known as magneto-plumbite structure), where A = Ba, Sr, Ca, or La and Me = a bivalent transition metal. Y-type hexaferrite phase that has the complex crystal structure ($Ba_2Me_2Fe_{12}O_{22}$) has been least studied. Few reports regarding the phase formation process, microstructure, magnetic properties and thermal characterization of Y-type hexaferrite had been reported [3-10]. Y-type hexagonal ferrites have planar magnetic anisotropy. Their cut-off frequency is higher than that of spinel ferrites [11]. Y-type hexagonal ferrite exhibits excellent magnetic properties in hyper-frequency. It is anticipated that the Y-type hexagonal ferrite will meet the need of soft magnetic materials for chip components in hyper frequency. Y-type hexagonal ferrite is an interesting material system for microwave application. Our works focus on the effect of substitution on structural and magnetic properties of Y-type hexaferrites.

2. Experimental

A series of polycrystalline $Ba_2Ni_{2-x}Zn_xFe_{12}O_{22}$ ($0.0 \le x \le 0.6$ *in the step of* 0.1) samples were synthesized using the

*Corresponding author.

standard solid state reaction technique. High purity (99.9%) powders of NiO, ZnO, Ba_2O_3 and Fe_2O_3, were mixed thoroughly in an appropriate amount. Mixing was performed in the ball mill in a wet medium to increase the degree of mixing. The mixed powders were calcined at 900˚C for 5 hours in air. The calcined powders were crushed into fine powders and toroid and disk shaped samples were prepared from these calcined powders using uniaxial pressure a press of 8×10^8 N/m^2. The samples were sintered at temperatures 1150˚C, 1200˚C and 1250˚C in air for 5 hours.

X-ray diffraction analysis was carried out using X-ray diffractometer equipped with CuKα radiation (λ = 1.5418 Å).

The frequency characteristics of the $Ba_2Ni_{2-x}Zn_xFe_{12}O_{22}$ ($0.0 \le x \le 0.6$ in the step of 0.1) hexaferrite samples *i.e.* the complex initial permeability spectra were investigated using Wayne Kerr Precision Impedance Analyzer (model No. 6500B). The complex permeability measurements on toroid shaped specimens were carried out at room temperature on all the samples in the frequency range 100 kHz - 120 MHz. The magnetization (M) measurements as a function of field at room temperature were made on pieces of the samples (approximate dimensions $2 \times 1 \times 1$ mm^3) using the Superconducting Quantum Interference Device (SQUID) magnetometer (MPMS-5S; Quantum design Co. Ltd.).

3. Results and Discussions

3.1. Structural Properties

The XRD patterns for various $Ba_2Ni_{2-x}Zn_xFe_{12}O_{22}$ ($0.0 \le x \le 0.6$ in the step of 0.1) Y-type hexagonal ferrites are shown in **Figure 1**. All peaks observed in the XRD patterns are identified with their Miller indices. The XRD patterns for these compositions confirm the formation of Y-type hexaferrite with a few impurity peaks [12]. The impurity peaks are mainly from the unreacted ingredients $BaCO_3$, NiO, ZnO and Fe_2O_3. The average values of the lattice parameters are calculated from the diffractograms using the formula [13]

$$\frac{1}{d_{hkl}} = \left[\frac{4}{3}\left(\frac{h^2+hk+k^2}{a^2}\right)+\frac{l^2}{c^2}\right]^{\frac{1}{2}} \quad (1)$$

where h, k and l are the indices of the crystal planes, d_{hkl} is the interplaner distance, and "a" and "c" are the lattice parameters. It is found that Y-type structure has average lattice parameters (a = 5.884 Å and c = 43.6 Å) that agree well with other author [4] for Ba Y-type hexaferrrites. The lattice parameters "a", and "c" of $Ba_2Ni_{2-x}Zn_xFe_{12}O_{22}$ compositions are plotted as a function of Zn content, as shown in **Figure 2**. From the figure it is observed that the lattice parameters "a" and "c" increase with Zn content in

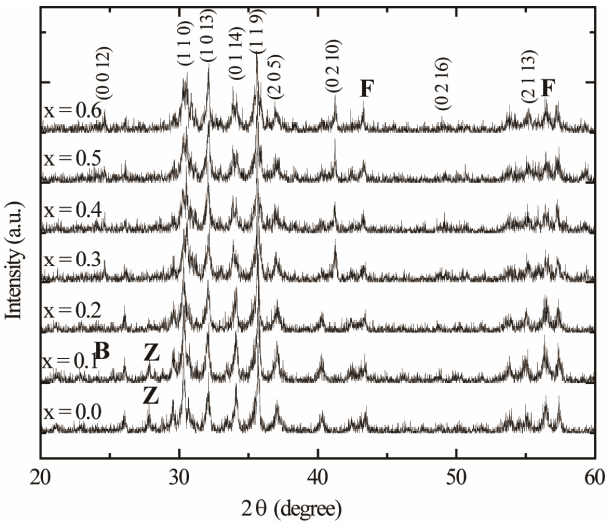

Figure 1. X-ray diffractogram (XRD) of various polycrystalline $Ba_2Ni_{2-x}Zn_xFe_{12}O_{22}$ samples sintered at 1200˚C (B: $BaCO_3$, Z: ZnO, F: Fe_2O_3).

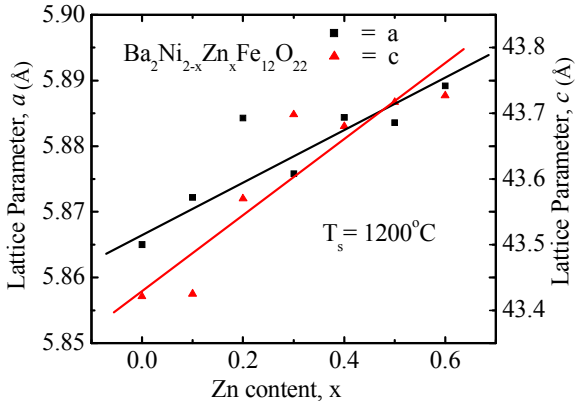

Figure 2. Variation of lattice parameter "*a*" and "*c*" with Zn content "*x*" of various polycrystalline $Ba_2Ni_{2-x}Zn_xFe_{12}O_{22}$.

the $Ba_2Ni_{2-x}Zn_xFe_{12}O_{22}$. The increase in lattice parameter with increasing Zn content can be explained on the basis of the ionic radii. The ionic radii of the cations used in $Ba_2Ni_{2-x}Zn_xFe_{12}O_{22}$ are 0.83Å (Ni^{2+}), 0.88Å (Zn^{2+}) and 0.69Å (Fe^{3+}) [14]. Since the ionic radius of Ni^{2+} is less than that of Zn^{2+}, increase in lattice parameter with the increase in Zn substitution is expected.

The theoretical density d_{th} is calculated using following expression [15]:

$$d_{th} = \frac{2nM}{\sqrt{3}N_A a^2 c}\ \mathrm{g/cm^3} \quad (2)$$

where n is the number of molecules per unit cell, N_A is Avogadro's number (6.02×10^{23} mol^{-1}), M is the molecular weight. **Figure 3** shows the variation of theoretical density (d_{th}) and bulk density (d_B) of the samples with Zn content sintered at 1200˚C. It is observed that the theoretical density increases slightly with increasing Zn

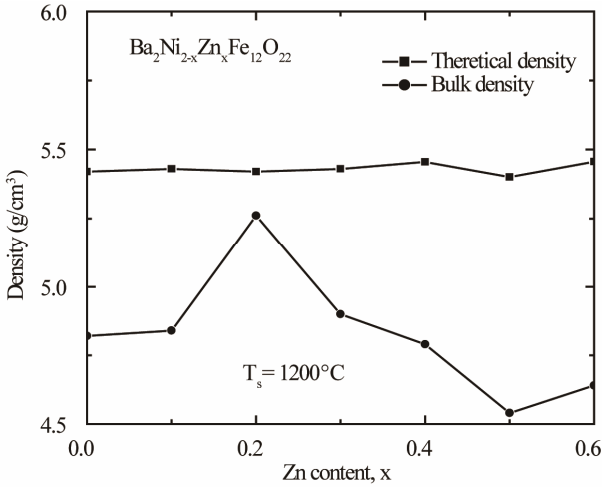

Figure 3. Variation of theoretical density (d_{th}) and experimental density (d_B) with Zn content "*x*" of various polycrystalline $Ba_2Ni_{2-x}Zn_xFe_{12}O_{22}$.

content with minute inconsistency. This increase in density with increasing Zn content can be explained on the basis of the atomic weight. Since the atomic weight of Ni (58.693 amu) is less than that of Zn (65.39 amu) there- fore increase in density is expected. The bulk density increases with Zn content up to x = 0.2 and then decreases. This decrease in density is attributed to the increased intra-granular porosity resulting from discontinuous grain growth as proposed by Coble and Burke [16].

The porosity is calculated from the relation $\{100(d_{th}-d_B)/d_{th}\}\%$, where d_B is the bulk density measured by the formula $d_B = M/V$ [16]. The bulk density and porosity as a function of Zn content of the samples sintered at 1200˚C is shown in **Figure 4**. It is observed that the bulk density increases with increasing Zn content in $Ba_2Ni_{2-x}Zn_xFe_{12}O_{22}$ up to a certain level (x = 0.2). This may be due to the formation of solid solution. It is supposed that all Zn^{2+} ions enter into the lattice during sintering and activating of the lattice diffusion. This assumption of the formation of solid solution is confirmed by the lattice constant measurement in which the lattice constant increases with Zn content.

The increase of the lattice constant usually increases the diffusion path, leading to an increase of the rate of cation interdiffusion in the solid solution. After the certain level (x > 0.2), density begins to decrease, this decrease in density is attributed to the increased intra-granular porosity resulting from discontinuous grain growth as proposed by Coble and Burke [16]. Porosity has the opposite trend.

3.2. Magnetic Properties

The frequency dependence of the complex permeability

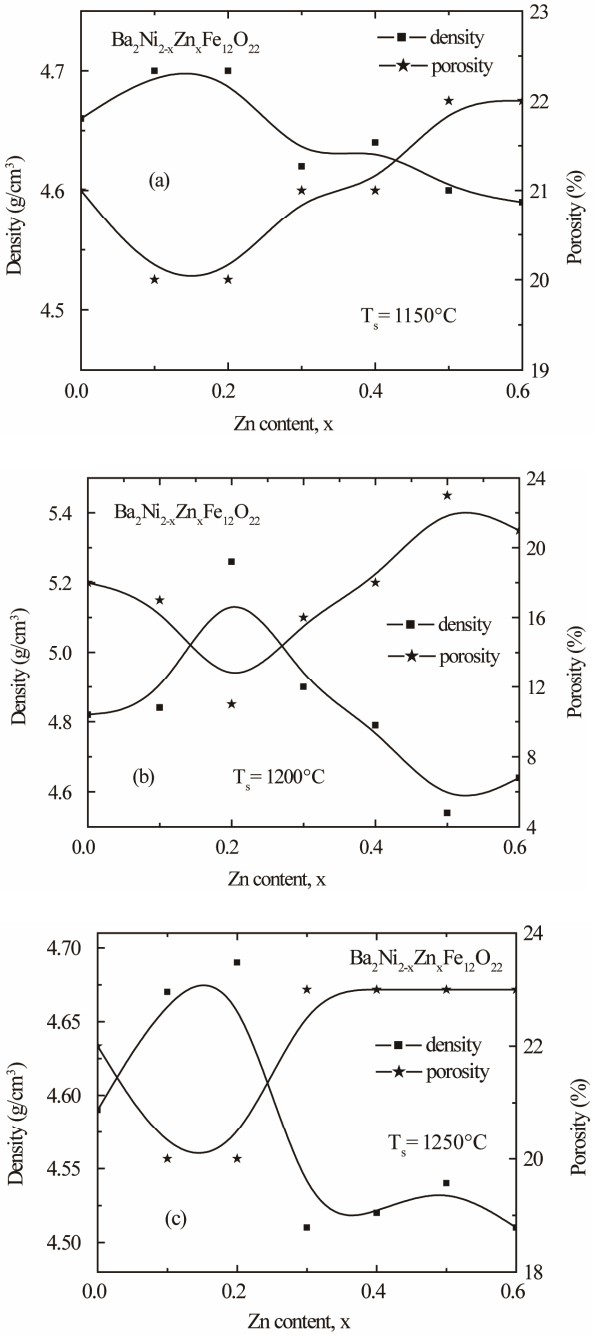

Figure 4. Variation of experimental density and porosity with Zn content "*x*" of various polycrystalline $Ba_2Ni_{2-x}Zn_xFe_{12}O_{22}$ sintered at (a) 1150˚C (b) 1200˚C and (c) 1250˚C.

of the samples sintered at 1200˚C is illustrated in **Figure 5** in the range from 100 kHz to 120 MHz. The real part (μ_i') and imaginary part (μ_i'') of the complex permeability are calculated using the following relations [17]: $\mu_i' = L_s/L_o$ and $\mu_i'' = \mu_i' \tan\delta$, where L_s is the self-inductance of the sample core and $L_o = \mu_o N^2 S/\pi\bar{d}$ is derived geometrically. Here L_o is the inductance of the winding coil without the sample core, N is the number of

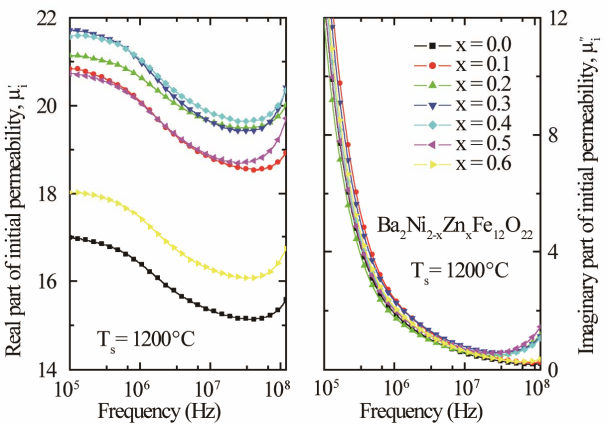

Figure 5. Real and imaginary part of initial permeability for various $Ba_2Ni_{2-x}Zn_xFe_{12}O_{22}$ sintered at 1200˚C for 5 h in air.

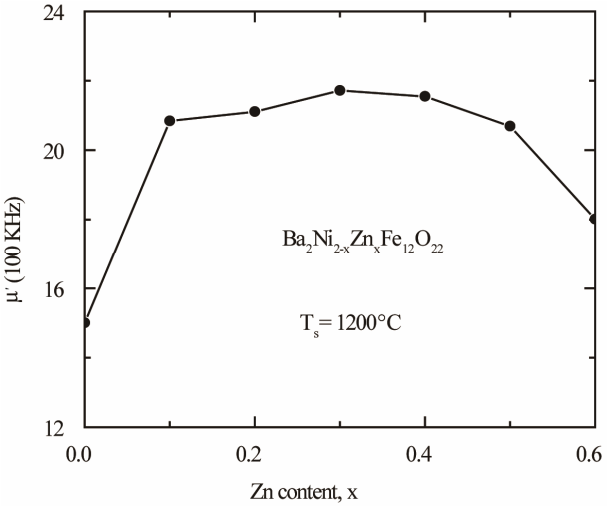

Figure 6. Variation of permeability for various $Ba_2Ni_{2-x}Zn_xFe_{12}O_{22}$ at 100 kHz with Zn Content sintered at 1200˚C for 5 h in air.

turns of the coil ($N = 5$), S is the area of cross section of the toroidal sample and $\bar{d}$ is the mean diameter of the sample. μ_i' decreases monotonically with frequency for all samples up to approximately 50 MHz. Similar results were observed for all the studied samples [18]. However, natural resonance phenomenon is not observed in μ_i' for any sample within measurement frequency range. This is because Y-type hexagonal ferrites have a cut-off frequency at GHz, about an order of magnitude higher than that of spinel ferrites [11]. The μ_i'' decreases with frequency for all the samples and this decrease is more rapid at low frequencies. There is a little increase of imaginary part (μ_i'') at a frequency higher than 50 MHz. The μ_i'' arises due to the lagging of the motion of the domain walls with the applied alternating magnetic field. This behaviour resembles a typical relaxation character. It may be due to reversible displacement of domain walls [19]. Initial permeability is found to increase significantly with the increase of Zn content up to a certain level and then decreases as depicted in **Figure 6**. The initial permeability of ferrite material depends on many factors like reversible domain wall displacement, domain wall bulging as well as microstructural features viz., average grain size, intra-granular porosity, etc. [11]. In a demagnetized magnetic material, there are a number of Weiss domains with Bloch walls separating two domains. These walls are bound to the equilibrium positions. It is well known that the permeability of polycrystalline ferrite is related to two magnetizing mechanisms: spin rotation and domain wall motion. [20], which can be described as follows:

$$\mu_i = 1 + \chi_w + \chi_{\text{spin}}$$

where χ_w is the domain wall susceptibility; χ_{spin} is intrinsic rotational susceptibility. χ_w and χ_{spin} may be written as: $\chi_w = 3\pi M_s^2 D/4\gamma$ and $\chi_{\text{spin}} = 2\pi M_s^2/K$ with M_s saturation magnetization, K the total anisotropy, D the average grain diameter, and γ the domain wall energy. Thus the domain wall motion is affected by the grain size and enhanced with the increase of grain size. The initial permeability is therefore a function of grain size. The magnetization caused by domain wall movement requires less energy than that required by domain rotation. As the number of walls increases with the grain sizes, the contribution of wall movement to magnetization increases.

Energy loss is an extremely important factor in ferromagnetic materials, since the amount of energy wasted on process other than magnetization can prevent the AC applications of a given material. The ratio of μ_i'' and μ_i' representing the losses in the material are a measure of the inefficiency of the magnetic system. Obviously this parameter should be as low as possible. The magnetic losses, which cause the phase shift, can be split up into three components: hysteresis losses, eddy current losses and residual losses. This gives the formula $\tan\delta_m = \tan\delta_h + \tan\delta_e + \tan\delta_r$. As μ_i is the initial permeability which is measured in presence of low field, therefore, hysteresis losses vanish at very low field strengths. Thus at low field the remaining magnetic losses are due to eddy current losses and residual losses. Residual losses are independent of frequency. Eddy current losses increase with frequency and are negligible at very low frequency. Eddy current loss can be expressed as $P_e \approx f^2/\rho$, where P_e is the energy loss per unit volume, f is the frequency and ρ is the resistivity [20]. To keep the eddy current losses constant as frequency is increased; the resistivity of the material chosen must increase with the square of frequency. The ferrite microstructure is assumed to consist of grains of low resistivity

separated by grain boundaries of high resistivity. Thicker grain boundaries are preferred to increase the resistance. The variation of loss factor, tanδ, with frequency in the range from 100 kHz to 120 MHz for the polycrystalline $Ba_2Ni_{2-x}Zn_xFe_{12}O_{22}$ compositions sintered at 1200˚C is shown in **Figure 7**. Loss factor decreases with frequency up to approximately 40 MHz and after that the loss factor increases with frequency. Therefore at higher frequency the loss is due to eddy current loss.

An intrinsic property such as saturation magnetization (M_s) is controlled by the composition whereas an extrinsic property, the microstructure, is in turns governed by the processing techniques. The magnetization of magnetic materials is a structural sensitive static property (intrinsic property), the magnetic field required to produce the saturation value varies according to the relative geometry of the field to the easy axes and other metallurgical conditions of the material. The magnetization as a function of applied magnetic field, *M-H*, for polycrystalline $Ba_2Ni_{2-x}Zn_xFe_{12}O_{22}$ samples at room temperature (300 K) is shown in **Figure 8**. The magnetization of $Ba_2Ni_{2-x}Zn_xFe_{12}O_{22}$ samples increases linearly with increasing the applied magnetic field up to 0.1 T and attains its saturation value for fields higher than 1.5 Tesla. In low field Rayleigh region, magnetization is believed to change entirely by domain wall motion. Between the low-field Rayleigh region and the high field region near saturation there exists a large section of the magnetization curve, comprising most of the change of magnetization between zero and saturation. The main processes occurring here are large Barkhausen jump, and the shape of this portion of the magnetization curve varies widely from one kind of specimen to another. In high field region, on the other hand, domain rotation is predominant effect, and this phenomenon obeys fairly simple rules. The variation of the saturation magnetization of the compositions with the Zn content is plotted in **Figure 9**. The highest saturation magnetization is obtained at x = 0.1. The increase of M_s with Zn content can be explained as: Fe^{3+} and Ni^{2+} ions are magnetic and the numbers of Bohr magnetons are 5 μ_B and 2 μ_B respectively, while Zn^{2+} is a kind of nonmagnetic ion [21]. The saturation magnetization of BaY ferrite at 0 K strongly depends on the distribution of these ions among the six different sublattice sites ($3a_{VI}$, $6c_{VI}$, $3b_{VI}$, $18h_{VI}$, $6c_{IV}$ and $6c_{IV}$*) [21]. It has been known that the $6c_{VI}$, $6c_{IV}$ and $6c_{IV}$* sites are spin-down, while the others are spin-up. The magnetic ions occupying the spin-up sites will provide positive magnetization, while the ions locating at the spin-down sites give negative magnetizations (the direction of

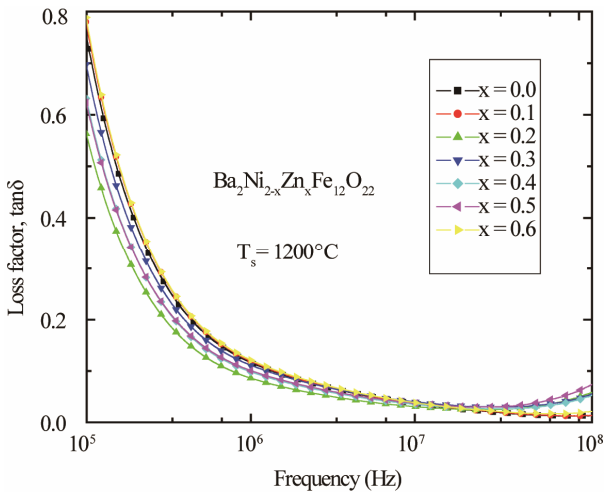

Figure 7. Variation of loss factors with frequency for various polycrystalline $Ba_2Ni_{2-x}Zn_xFe_{12}O_{22}$ sintered at 1200˚C.

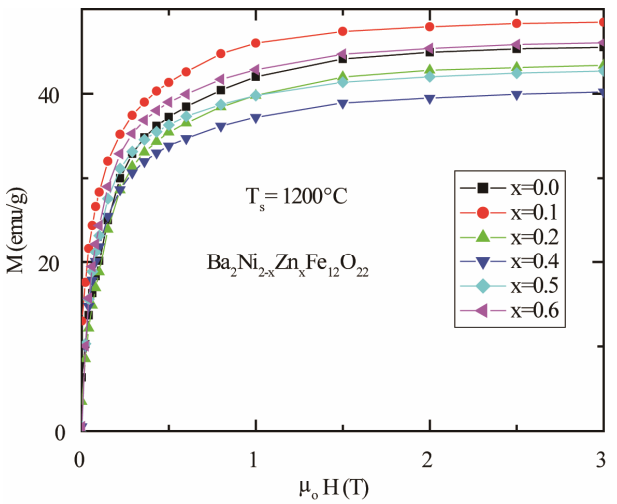

Figure 8. The magnetization as a function of applied magnetic field at 300 K for various polycrystalline $Ba_2Ni_{2-x}Zn_xFe_{12}O_{22}$ sintered at 1200˚C.

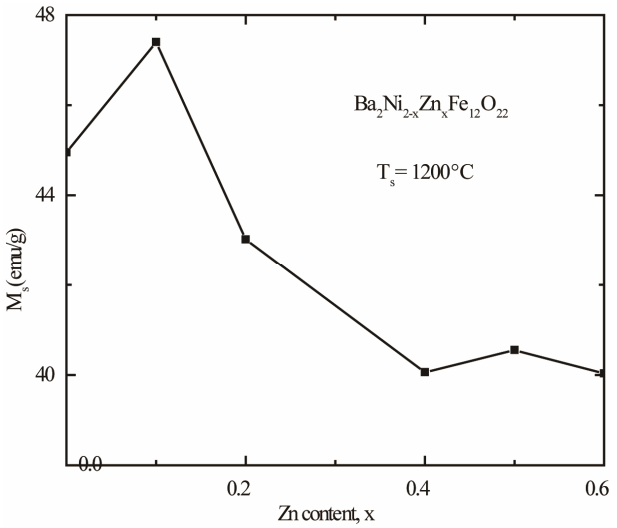

Figure 9. Variation of saturation magnetization for various polycrystalline $Ba_2Ni_{2-x}Zn_xFe_{12}O_{22}$ with zinc content, x sintered at 1200˚C.

magnetization is opposite to the applied magnetic fields). Nonmagnetic ions Zn^{2+} locating at $6c_{VI}$, $6c_{IV}$ and $6c_{IV}$* sites lead to a decrease in the negative magnetization, and thus increase net or total magnetization. Near room temperature, the saturation magnetization M_s will decrease more rapidly for the samples with higher Zn concentration on account of the effect of thermal agitation. Hence, M_s decreases rapidly when Zn concentration is higher than 0.1.

4. Conclusion

The XRD patterns for the polycrystalline $Ba_2Ni_{2-x}Zn_xFe_{12}O_{22}$ ($0.0 \leq x \leq 0.6$ in the step of 0.1) compositions confirm the formation of Y-type hexaferrites. Lattice parameter increases with increasing of Zn content for almost all the compositions. The ionic radius of Ni^{2+} is less than that of Zn^{2+} and increase in lattice parameters with the increase in Zn substitution is expected. The bulk density of the samples increases and the corresponding porosity of the samples decreases with increasing of Zn content up to x = 0.2 and then both factors decrease. Initial permeability value increases with increasing Zn content and maximum at x = 0.3. It is observed from permeability vs. frequency curves that the natural resonance phenomenon is not observed in μ_i' within measurement frequency range. This implies that their cut off frequency lies in the high frequency region. Therefore it can be used for microwave application. From the *M-H* curve it is clear that at room temperature the polycrystalline $Ba_2Ni_{2-x}Zn_xFe_{12}O_{22}$ compositions are in ferrimagnetic state.

5. Acknowledgements

The present study was supported by CASR, Bangladesh University of Engineering and Technology (BUET). The authors would like to thank Prof. Tomoji Kawai of ISIR, Osaka University, Japan, for allowing them to use his laboratory facilities.

REFERENCES

[1] J. Kulikowski, "Soft Magnetic Ferrites-Development or Stagnation," *Journal of Magnetism and Magnetic Materials*, Vol. 41, No. 1-3, 1984, pp. 56-62. doi:10.1016/0304-8853(84)90136-7

[2] R. S. Devan, Y. D. Kolekar and B. K. Chougule, "Effect of Cobalt Substitution on the Properties of Nickel-Copper Ferrite," *Journal of Physics*: *Condensed Matter*, Vol. 18, No. 43, 2006, pp. 9809-9821. doi:10.1088/0953-8984/18/43/004

[3] Y. Bai, J. Zhou, Z. Gui and L. Li, "Preparation and Magnetic Chacterization of Y-Type Hexaferrites Containing Zinc, Cobalt and Copper," *Materials Science and Engineering B*, Vol. 99, No. 1, 2003, pp. 266-269.

[4] Y. Bai, J. Zhou, Z. Gui, Z. Yue and L. Li, "Phase Formation Process, Microstructure and Magnetic Properties of Y-Type Hexagonal Ferrite Prepared by Citrate Sol-Gel Auto-Combustion Method," *Materials Chemistry and Physics*, Vol. 98, No. 1, 2006, pp. 66-70.

[5] R. C. Lima, M. S. Pinho and T. Ogasawara, "Thermal Chacterization of the Intermediary Products of the Synthesis of Zn-Substituted Barium Hexaferrite," *Journal of Thermal Analysis and Calorimetry*, Vol. 97, No. 1, 2009, pp. 131-136.

[6] Y. Bai, J. Zhou, Z. Gui and L. Li, "Magnetic Properties of Non-Stoichiometric Y-Type Hexaferrite," *Journal of Magnetism and Magnetic Materials*, Vol. 250, 2002, pp. 264-269.

[7] A. Deriu, F. Licci, S. Rinaldi and T. Besagni, "Y-Type Hexagonal Ferrites Containing Zinc, Copper and Cadmium: Magnetic Properties and Cation Distribution," *Journal of Magnetism and Magnetic Materials*, Vol. 22, No. 3, 1981, pp. 257-262. doi:10.1016/0304-8853(81)90030-5

[8] Y. Bai, J. Zhou, Z. Gui, L. Li and L. Qiao, "The physic Properties of Bi-Zn Codoped Y-Type Hexagonal Ferrite," *Journal of Alloys and Compounds*, Vol. 450, No. 1-2, 2008, pp. 412-416. doi:10.1016/j.jallcom.2006.10.122

[9] Z. Haijun, J. Xiaolin, Y. Xi and Z. Liangying, "Manufacture of Zn-Co Substituted Y-Type Barium Hexagonal Ferrites by Citrate Precursor Route and Their Microwave Properties," *Journal of Rare Earths*, Vol. 22, No. 3, 2004, p. 338.

[10] F. Bolzoni and L. Pareti, "Magnetic Properties of Y-Type Trigonal Ferrites First Order Magnetization Processes in Trigonal Systems," *Journal of Magnetism and Magnetic Materials*, Vol. 42, No. 1, 1984, pp. 44-52. doi:10.1016/0304-8853(84)90288-9

[11] J. Smit and H. P. J. Wijn, "Ferrites," Cleaver-Hume Press, London, 1959.

[12] Y. Bai, J. Zhou, Z. Gui, Z. Yue and L. Li, "Preparation and Magnetic Characterization of Y-Type Hexaferrites Containing Zinc, Cobalt and Copper," *Materials Science and Engineering*: *B*, Vol. 99, No. 1-3, 2003, pp. 266-269. doi:10.1016/S0921-5107(02)00545-7

[13] X. Liu, W. Zhong, S. Yang, Z. Yu, B. Gu and Y. Du, "Influences of La^{3+} Substitution on the Structure and Magnetic Properties of M-Type Strontium Ferrites," *Journal of Magnetism and Magnetic Materials*,, Vol. 238, No. 2-3, 2002, pp. 207-214. doi:10.1016/S0304-8853(01)00914-3

[14] J. E. Huheey, E. A. Keiter and R. L. Keiter, "Inorganic Chemistry Principles of Structure and Reactivity," 4th Edition, Prentice Hall, Upper Saddle River, 1997.

[15] F. G. Brockman, P. H. Dowling and W. G. Steneck, "Dimensional Effects Resulting from a High Dielectric Constant Found in a Ferromagnetic Ferrite," *Physical Review*, Vol. 77, No. 1, 1950, pp. 85-93. doi:10.1103/PhysRev.77.85

[16] R. L. Coble and J. E. Burke, "Sintering in Ceramics, Progress in Ceramic Science," Pergamon Press, New York, 1964.

[17] A. A. Sattar, H. M. El-Sayed, K. M. El-Shokrofy and M. M. El-Tabey, "Improvement of the Magnetic Properties of Mn-Ni-Zn Ferrite by the Non-Magnetic Al^{3+} Ion Sub-

stitution," *Journal of Applied Sciences*, Vol. 5, No. 1, 2005, pp. 162-168.

[18] H. P. J. Wijn, "Hexagonal Ferrites," In: K.-H. Hellwege, Ed., *Landolt-Börnstein Numerical Data and Functional Relationships in Science and Technology New Series*, Spinger, New York, 1970, p. 558.

[19] R. Lebourgeois, J. P. Ganne and B. Llort, "High Frequency Mn-Zn Power Ferrites," *Journal de Physique IV France*, Vol. 7, No. C1, 1997, pp. 105-108. doi:10.1051/jp4:1997131

[20] T. Tsutaoka, M. Ueshima, T. Tokunaga, T. Nakamura and K. Hatakeyama, "Frequency dispersion and Temperature Variation of Complex Permeability of Ni-Zn Ferrite Composite Materials," *Journal of Applied Physics*, Vol. 78, No. 6, 1995, pp. 3983-3991. doi:10.1063/1.359919

[21] S. G. Lee and S. J. Kwon, "Saturation Magnetizations and Curie Temperatures of Co-Zn Y-Type Ferrites," *Journal of Magnetism and Magnetic Materials*, Vol. 153, No. 3, 1996, pp. 279-284. doi:10.1016/0304-8853(95)00559-5

